8-17-2020

Soil Moisture and Permittivity Estimation

Abdul Salam
Purdue University, salama@purdue.edu

Usman Raza
Purdue University

Chapter 9
Soil Moisture and Permittivity Estimation

Abstract The soil moisture and permittivity estimation is vital for the success of the variable rate approaches in the field of the decision agriculture. In this chapter, the development of a novel permittivity estimation and soil moisture sensing approach is presented. The empirical setup and experimental methodology for the power delay measurements used in model are introduced. Moreover, the performance analysis is explained that includes the model validation, and error analysis. The transfer functions are reported as well for soil moisture and permittivity estimation. Furthermore, the potential applications of the developed approach in di erent disciplines are also examined.

9.1 Introduction

IOUT can be applied to many fields of precision agriculture [1], [52], [24], [58], [9], [75], [100], [104] [50] . It is being used to provide important information to the farmers. IOUT has an ability to estimate soil properties and monitor soil moisture. An important component of precision agriculture applications (e.g., making real-time agricultural decision, smart agriculture variable rate irrigation (VRI), and water conservation) is continuous soil moisture sensing [14, 55]. Permittivity plays an important role in propagation analysis of electromagnetic (EM) waves on the basis of soil medium, depth, UG localization and subsurface imaging. Therefore, efficient measurement techniques for soil in-situ properties is very important. Method to determine soil permittivity includes: ground-penetrating radar (GPR) measurements [5], [13], [28], time-domain reflectometry (TDR) [25], [29, 58], [67], and remote sensing [18], [59], [68], [69]. Furthermore, disadvantage of laboratory method os estimating permittivity is o -line measuring the soil sample, and that of remote sensing is limitations of depth up to 20cm. In-situ methodologies can be used to measure soil properties for higher depths and that too with accuracy.

This chapter focus on developing an in-situ technique, Di-Sense, for measuring soil moisture and permittivity based on wireless underground communications (WUC) in

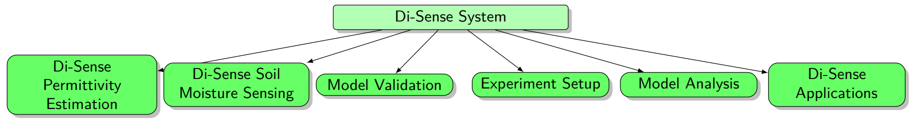

Fig. 9.1: Organization of the Chapter

IOUT. When EM waves propagates through the soil they are e ected by the distance, depth, frequency, soil moisture [46, 145] and soil properties [6]. Path loss at receiver can be used to determine the properties change of propagating signal. The approach in this chapter uses path for measuring permittivity and moisture of the soil. Path loss is highly dependent upon depth, distance and soil moisture. Di-Sense uses a buried transmitter antenna (fixed depth) for transmitting wideband signal using the frequency range of $100\,\mathrm{MHz}$ to $500\,\mathrm{MHz}$ and received signal is analyzed for measuring path loss. Di-Sense allows IOUT system to communicate and estimate permittivity and soil moisture sensing simultaneously. A model is developed to measure soil moisture and permittivity using path loss and is validated in an indoor testbed and a software defined radio (SDR) testbed. For validation, various soil parameters (depth, type and moisture level) are changed to study the impact of those parameters.

There has been lot of work done previously for determining soil permittivity and moisture. The literature review in this chapter is will try to cover only the most recent work and try to identify the similarities and di erences between the work. The process of estimating permitivity and soil water can be classified into two main approaches. For soil water estimation, TDR, gravimetric method, capacitance probes, GPR, hygrometric techniques, remote sensing, electromagnetic induction, neutron thermalization, tensionmetry, nuclear magnetic resonance, gamma ray attenuation, optical methods and resistive sensors can be used. Some of these approaches are discussed below. First estimation technique is soil properties based. Authors in [12] derives EM parameters of soil on the basis of soil moisture, frequency and soil density, however, the model has limitation of working with 20% soil moisture weight and also needs rigorous sample preparation. In [6, 37, 39], a probe-based equipment is developed for the laboratory use. The probe works with vector network analyzer (VNA) in frequency range of $45\,\mathrm{MHz}$ to $26.5\,\mathrm{MHz}$. In [74], author propose a model to calculate the dielectric soil permittivity o the basis of empirical evaluations. Similarly, a dielectric model for soil properties is developed by [7]. This model works for frequencies > 1.44 Mhz. Peplinski extended the model for characterization of dielectric behavior of soil under frequency range of 300 MHz to 1.3 GHz [26, 38, 42]. [6] extensively reviews the techniques for estimating soil permittivity. These method involves taking sample for laboratory measurements and are labor extensive. The laboratory sample technique does not depict the in-situ soil conditions. Hence, there is a need of automated approaches for monitoring soil moisture.

Another approach is given by [25] which uses TDR for measuring soil properties. It needs to measure refractive index and impedance of the soil. Authors in [67] uses Cross-Well Radar (CWR) to determine EM properties of soil. The purpose of the methodology is to detect Dense Non-Aqueous Phase Liquids (DNAPLs) hazardous materials. A wideband wave is transmitted under the frequency range of 0.5 GHz to 1.5 GHz. Transmission simulations and reflection is used to measure soil permittivity in dry sand. [27, 30, 70] extensively reviews such time domain-based techniques for estimating soil permittivity. In TDR-based approaches, sensors are place at each location where measurements are needed. However, it is important to obtain real-time soil moisture sensing data so that e ective decision making can be achieved in agricultural applications.

Third category of estimating soil properties falls under the antenna based approaches. [60] and [61] propose a method of measuring electrical properties of the earth using buried antennas. However, length of antenna is adjusted so that the input reactance remains zero. [62] uses Fresnel reflection coefficient to measure the soil permittivity on the basis of GPR measurements. However, the result in this study are without any empirical validation and also needs to be analyzed in time-domain. Authors in [3] measures soil dielectric properties for frequency range of 0.1-1 GHz. They use wideband frequency domain method and needs LCR meter for measuring impedance and VNA. Complex dielectric properties are measured in frequency domain by using probes [24], [36, 75].

In [13], GPR based technique is utilized for permittivity estimation by correlating cross-talk of GPR signal and dielectric properties of soil. However, GPR methods are only applied for the implementations which requires calibration and low depths (0-20 cm).

Measurements from remotes sensing methods has wider range [69], but are more susceptible soil water content [18]. Remote sensing methods are classified into active and passive remote sensing [20]. Passive techniques have low spatial resolution (in the order of kilometers) and active has high spatial resolution (in the order of meters). However, with active methods measurements values are limited to few centimeters of topsoil layer and its accuracy is also e ected by vegetation cover [59].

This review of measurement methods identify the gap between large scale and point-based measurements which can be covered by WUC. The chapter focus on using WUC for permittivity and soil moisture estimation. It is known that soil properties and soil moisture impacts the EM waves propagating through soil [139], [145], hence, even a small amount of water can highly e ect the IOUT wireless channel between transmitter and receiver. Analysis of path loss at receiver give a more detailed idea about these changes. This method can use the field IOUT infrastructure without using soil moisture sensors. Therefore, WUC are successfully being used for soil sensing. Last decade has seen significant improvement in various aspect of IOUT communication such as UG communications, characterization of impact of soil type and moisture, and UG channel modeling [1], [58], [9], [75], [100], [50], [145], [170], [104], [31, 45, 71]. Authors in [26, 145] characterize the wireless UG channel in a very detailed manner. Similarly, [139] studies the impact of soil moisture and soil type on the capacity of multi-carrier modulations and also validate the results empirically. To the best of our knowledge, no study provide WUC-based in-situ estimation of these properties in real-time. Therefore, this will be the first work to estimate soil

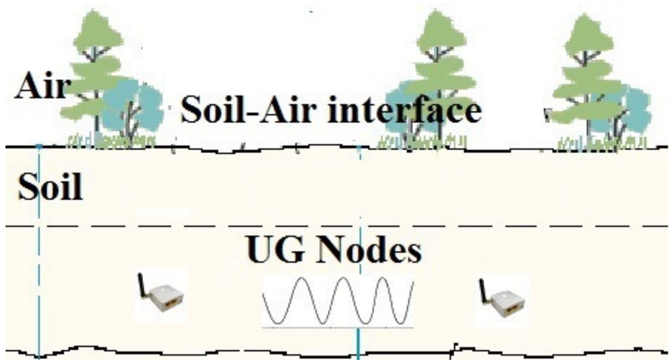

Fig. 9.2: WUC implementation for determining soil properties [55]

permittivity and soil moisture in response to channel path loss and velocity of Em wave in UG channel.

Table 9.1: Antenna depths, VWC percentage, and particle distribution for di erent types of soil used in a testbed

Textural Class	Sand (%)	Silt (%)	Clay (%)	VWC Range (%)	Depth
Silty Clay Loam - Greenhouse (SCL-G)	13	55	32	32 - 38	20 cm
Silt Loam - Field (SL-F)	17	55	28	22 - 38	10, 20, 30, and 40 cm
Sandy Soil - Indoor Testbed (S-I)	86	11	3	15 - 38	10, 20, 30, and 40 cm
Silt Loam - Indoor Testbed (SL-I)	33	51	16	30 - 37	10, 20, 30, and 40 cm

9.2 System Models

Expression are derived for calculating soil permittivity and soil moisture at the distance of 1m - 15m. These expressions connects both of the soil parameters to WUC. It is connected to propagation path loss and wave velocity for calculating permittivity. TO that end, problem is formulated as follow: Derive a function for calculating soil permittivity and soil moisture as an output for an input of path loss of the link to the system. Fig. 9.2 shows the schema of WUC along with the sensing UG nodes. For a low electrical loss, there is no di erence between the e ective permittivity and complex permittivity. This chapter refer the the permittivity as a relative permittivity. Section 9.2.1 discuss the Di-Sense permittivity estimation and Section 9.2.2 discuss the soil moisture model.

9.2.1 Di-Sense Permittivity Estimation

Propagation Path Loss Approach: IOUT communication is mainly carried out through EM waves propagation in the soil. The propagation loss of the EM waves due to water in the soil is highly dependent upon the real e ective permittivity, i.e., dielectric constant of the soil. Therefore, it is possible to use the propagation loss for calculating soil moisture (within the range of 100MHz - 500MHz) and relative permittivity. For modeling the permittivity of the soil, a known signal is transmitted using narrow bandwidth. A lowest path loss (LPL) is calculated for the signal among all frequency ranges and frequency is increased sequentially in predefined intervals, Δf. The propagation loss of the received signal is measured at the receiver end. Path loss can be defined as the ratio of transmit signal power at sender $P_t$to the received signal at the receiver P_r. It is given as as follow:

$$PL = P_t - P_r = 10. \log 10(P_t/P_r) \;, \tag{9.1}$$

where denotes system path loss, along with the e ects of both antenna gains, i.e., transmitting G_t and receiving G_r. After measuring the path loss, the frequency of the lowest path loss is calculated as follow:

$$f_{min} = F(\min(PL(f))) \;, \tag{9.2}$$

where f_{min} represents the frequency of the minimum path loss. The distance between the transmitting and receiving antenna has no e ect on f_{min} due to antennas gains. Therefore, PL already contains the antenna gains. Since narrowband is used for calculating PL measurements, noise e ects in the signal are minimal. Next the soil factor, ϕ, is given as follow:

$$\phi_s = f_{min}/f_0 \;, \tag{9.3}$$

where f_0 denotes the resonant frequency of the antenna in the free space. After calculating the soil factor ϕ_s, the wavelength at frequency f_0 is calculated as follow:

$$\lambda_0 = c/f_0 \;, \tag{9.4}$$

where c is the speed of light. Relative permittivity of the soil is calculated as:

$$\epsilon_r = \frac{1}{(\phi_s \times \lambda_0)^2} \;. \tag{9.5}$$

Permittivity Estimation through Velocity of Wave Propagation in Soil: Soil permittivity varies greatly because of it being non-homogeneous characteristics which results in variation in phase velocity and wavelength of the signal as it propagates through the soil[53]. Therefore, the velocity of the signal can also be used to calculate the permittivity of the soil. Power delay profile (PDP) is known by the geometry layout of the testbed which in turn is used to measure the velocity of the signal. Direct wave component travels completely through the soil. Hence, After calculating the signal velocity, C_s, di erence between the arrival and transmission time of direct

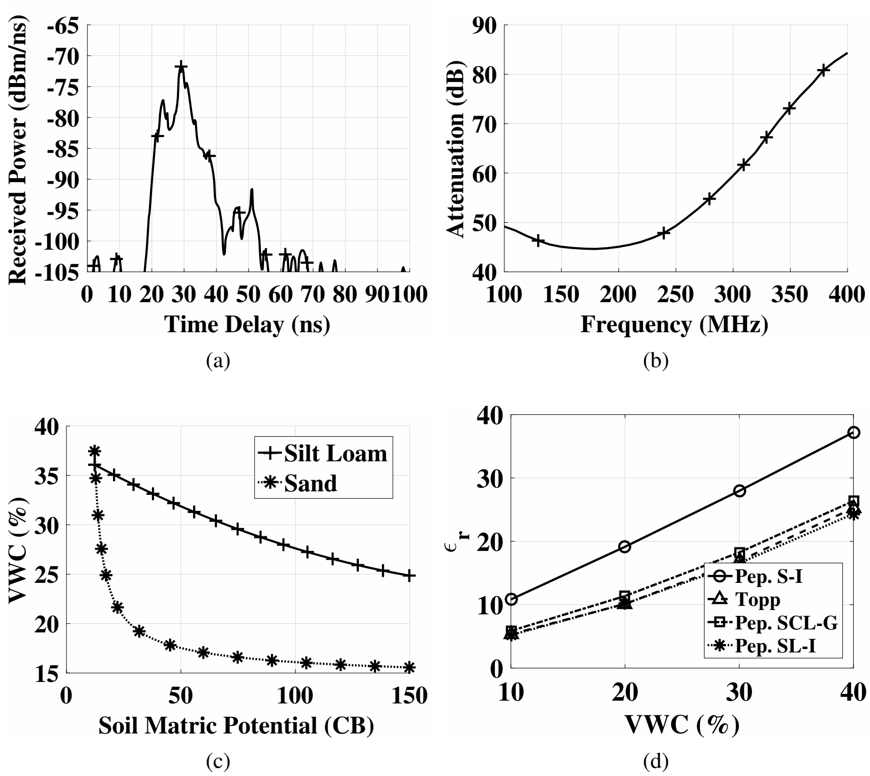

Fig. 9.3: (a) Power delay profile (PDP) (Silt Loam Soil and Indoor Testbed), (b) Signal attenuation in soil with changing operational frequency, (c) Conversion of soil matric potential to VWC [15, 16], (d) Relation between VWC and soil permittivity as per Topp and Peplinski model [27, 55]

wave component is used to measure the relative permittivity. Consequently, ϵ_r is calculated as follow:

$$\epsilon_r = \left[C_s \times \frac{(\tau_{dr} - \tau_{dt})}{l}) \right] , \tag{9.6}$$

where the distance between receiver and transmitter antennas is given as l, travel time of the direct component in the soil is given as $\tau_{dr} - \tau_{dt}$, and the wave propagation velocity in soil is denoted by C_s. Propagation velocity of wave id di erent in soil and air. Due to this di erence the direct wave has lower attenuation as compared to lateral wave and travels along the soil-air interface through air.

Figs. 9.3, as an example, gives PDP in silt loam soil. It plots the soil attenuation with operational frequency.

9.2.2 Di-Sense Soil Moisture Sensing

Soil moisture-permittivity relation is no dependent upon bulk density, soil texture, and frequency[66]. It is possible to determine the soil water content from soil permittivity as soil moisture is only dependent upon the soil permittivity [19], [66] [1]

Relative permittivity of the dry soil is 3 and that of water is 80, therefore, it is calculating by equation (9.5) and (9.6) and soil moisture is calculated as given in [19], [66]:

$$VWC(\%) = \frac{\epsilon_r - 3}{.77} + 14.97\,. \tag{9.7}$$

9.3 Model Validation Techniques

Soil moisture sensors are used to measure the soil water content and validate the model. Two main methods used to represent the soil water content are: volumetric water content (VWC) and soil matric potential (SMP). Watermark sensors are used for measurement of SMP in centibars (CB)/kilopascals (kPa)[2]. Soil-water retention curve in [15, 28] is used to convert soil matric potential to soil volumetric water content (VWC). Fig. 9.3(c) shows the water retention curves for silt loam soil and sandy soil. For sandy soil, SMP is inversely proportional to VWC and a small increase in SMP causes the VWC to drop significantly because of large pore size[17, 43]. Therefore, developing soil texture-based water-retention curves for di erent soil types with varying soil moisture levels is very important [16, 34].

In addition to these sensor measurements, Peplinski's dielectric and Topp's model is also used to validate the Di-Sense model. This validation is performed with di erent soil types and soil water content. Soil type has no e ect on Topp model [34, 66], and it related soil water content to soil permittivity. Topp model is given as follow:

$$\theta = 4.3 \times 10^{-6}\epsilon^3 - 5.5 \times 10^{-4}\epsilon^2 + 2.92 \times 10^{-2}\epsilon - 5.3 \times 10^{-2} \tag{9.8}$$

where θ represents the soil water content, and ϵ represents the dielectric constant of the soil.

Soil dielectric constant is measured by the Peplinski model [26]. Soil dielectric constant is given as $\gamma = \alpha + j\beta$ where,

---

[1] Soil moisture-permittivity relation is proved to work in coarse textured soils and fine textured soil, however, some error were found in the relationship and this relation is weak in mineral soils [21, 55].

[2] Higher matric potential values equals low soil moisture and, similarly, near saturation point is denoted by zero matric potential 1 CB = 1 kPa.

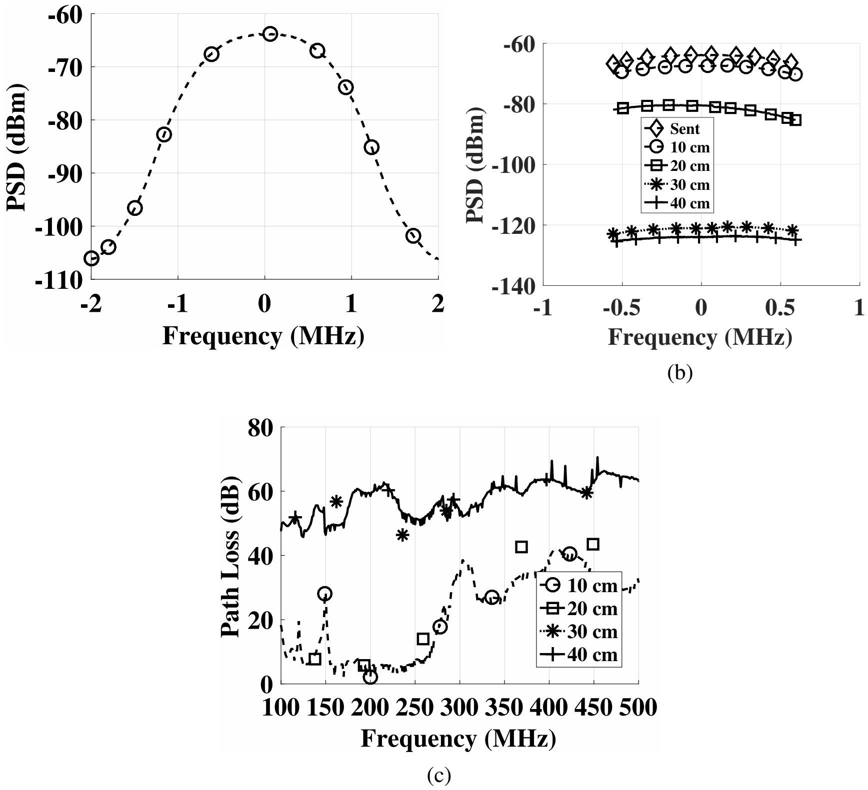

Fig. 9.4: Power spectral density [55]: (a) Transmitted signal, (b) Received signal; and (c) E ect of frequency on Path loss [55]

$$\alpha = \omega \sqrt{\frac{\mu\epsilon'}{2}\left[\sqrt{1+(\frac{\epsilon''}{\epsilon'})^2}-1\right]}\,, \tag{9.9}$$

$$\beta = \omega \sqrt{\frac{\mu\epsilon'}{2}\left[\sqrt{1+(\frac{\epsilon''}{\epsilon'})^2}+1\right]}\,, \tag{9.10}$$

where μ is the magnetic permeability, $\omega = 2\pi f$ is the angular frequency, and ϵ' and ϵ'' denotes the real and imaginary parts of the dielectric constant. Fig. 9.3(d) plots the relation between VWC and permittivity given by Topp and Peplanski model. Peplanski model is used for three di erent soil types whereas Topp model is independent of soil type.

9.4 Experiment Setup

This section discuss the experiment setup and methodology used for the validation of the model. Table 9.1 lists the values for burial depths, empirical VWC range, testbed classification and particle size distribution. For rest of the chapter, soil's name abbreviation are also used as given in Table 9.1.

9.4.1 Experiment Methodology

SDR testbed uses USRPs [9] and GNU Radio [10] for experiments. A UG dipole antenna buried at 40 cm are used to transmit Gaussian signal of 2 MHz bandwidth via transmitter USRP. Receiver USRPs receives the signal which is connected to dipole antennas buried at di erent depths of 10 cm, 20 cm, 30 cm, and 40 cm whereas the distance between the transmitter and receiver is fixed at 50 cm. Several experiments are performed for all depths and distances of 2 & 4 meters [44, 65]. For a given frequency, signal is transmitted by the transmitter for just one second and receivers receive IQ data of 4 mega samples. Transmitter transmit for the next frequency only after receiving the acknowledgment form the receiver. This done for all the frequency in the range of $100\,\mathrm{MHz}$ to $500\,\mathrm{MHz}$ at each depth and distances. Finally, three measurements are taken and Matlab[23] is used for the post-processing.

Welch's method [47, 76], an advanced form of periodogram analysis, is used for path loss analysis and spectral estimation. It uses Discretye Fourier Transform to divide the data into fixed blocks for calculation and modification of periodogram which are averaged out for estimating power spectrum. Fig. 9.4(a) shows the periodogram of the transmitted signal.

Fig. 9.4(b) shows the PSD for all depths at a distance of 50cm and the burial depth of the transmitter is 40cm, hence, shows that PSD is inversely proportional to the burial depths.

Fig. 9.4(b) shows the path loss for all depths. It can be observed that path loss is directly proportional to the burial depths, i.e., increase with the increase in frequency. Therefore, lower frequency, normally < 500 MHz, works better in WUC channel.

9.4.2 Power Delay Profile Measurements

The purpose of measuring PDP is to estimate the velocity of propagating wave. To that end, Keysight Technologies N9923A FieldFox VNA is used for measuring PDP. Experimental setup of indoor testbed is used for the purpose with sandy and siltloam soils, varying burial depths (10 cm, 20 cm, 30 cm, and 40 cm). For greenhouse testbed, silty clay loam soil and depth of 20cm is used with OTA resonant frequency of 433MHz for all types of soil. Finally, PDP and channel transfer function is measured for changing soil moisture levels [27, 55].

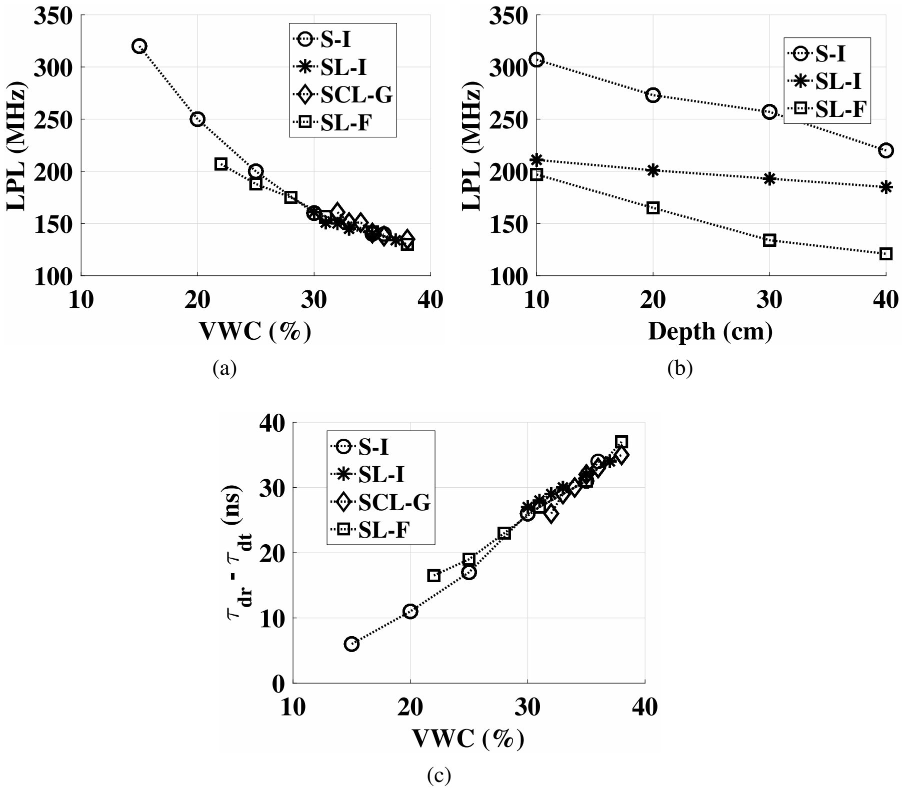

Fig. 9.5: VWC e ect, in di erent soil types, on [55]: (a) Lowest path loss frequency, (b) Depth, and (c) Wave velocity

For PDP measurement, VNA transmits a sinusoidal signal with frequency increasing in incremental increment. This frequency domain data is used to obtain the time-domain equivalent impulse response, $h(t)$, through inverse Fourier transform (IFFT). To that end, 401 complex tones are stored in range of $10\,\mathrm{MHz}$ - $4\,\mathrm{GHz}$, and sidelobes are suppressed by windowing the impulse response of the channel. The velocity is then calculated by the process in Section 9.2.

9.5 Model Analysis: Performance, Validation and Error

This section analyze the performance of the model and validate it. Section 9.5.1 discuss the impact of soil moisture, burial depth and soil moisture on path loss calculated by using the methodology described in Section 9.2. Section 9.5.2 provides the model validation and Section 9.5.3 perform the error analysis for the model.

9.5.1 WUC Path Loss

Figs. 9.5 shows the change in lowest path loss frequency of UG channel. The results are shown for three soil types: silt loam, silty clay loam, and sandy soil (Fig. 9.5(a)), varying soil moisture (Fig. 9.5(b)) and burial depth (Fig. 9.5(c)). It can be seen in Fig. 9.5(a) that for sandy soil, increase in soil moisture (15% to 36%) causes 56% decrease in lowest path loss frequency. For silt loam soil, increase in soil moisture (38% to 22%) causes 60% decrease in lowest path loss frequency and for silty clay loam soil this decrease is 15.62% for 32% to 38% increase in soil moisture. Generally, it can be concluded that lowest path loss is inversely proportional to soil moisture for these soil types. This is because of the fact that soil permittivity is greater than that of air causing it to increase with increasing soil moisture, hence, decreasing lowest path loss [49, 50, 52].

In Fig. 9.5(b) change in frequency loss is plotted for all three soil type under di erent burial depths. For silt loam soil, the lowest path frequency is decreased 12.32% as depth increases from 10cm to 40cm. For silt loam soil, the lowest path frequency is decreased by 12.32% (from $211\,\mathrm{MHz}$ to $185\,\mathrm{MHz}$) as depth increases from 10cm to 40cm, and that for silt loam soil (field) it decreases by 38% (from $197\,\mathrm{MHz}$ to $121\,\mathrm{MHz}$). Similarly, for sandy soil, the lowest path frequency is decreased by 28.24% (from $308\,\mathrm{MHz}$ to $221\,\mathrm{MHz}$) as depth increases from 10cm to 40cm. The reason for this behavior of lowest frequency is that wave reflected form the soil-air interface produces a current at antenna causing impedance to change, hence, resulting in lowest path loss frequency to change. The distance between soil-air interface increases with the increase in depth, therefore, the reflected waves attenuates because of high absorption rate of the soil. As the relative permittivity is directly proportional to the water content [7, 45], therefore, the change in lowest path loss frequency is greater in sandy soil than silt loam soil because silt loam soil high capacity of holding water. Sandy soil has lower permittivity causing the lowest path frequency shift to higher spectrum.

Fig. 9.5(c) plots the arrival time of direct wave component along with the changing soil moisture. It can be seen that velocity of the wave is inversely proportional to the soil moisture. The velocity decreases with the increasing soil moisture for all type of soil. Wave velocity decreases by five times for soil moisture increase of 15% to 36%, and for sil loam soil, it decreases three times for soil moisture increase of 22% to 38% [71, 72].

9.5.2 Validation

This section discuss the results for model validation. Equations (9.5), (9.6) and (9.7) are used to calculate the values for soil permittivity and soil moisture and are shown in Figs. 9.6. Figs. 9.6(a)-9.6(b) compares the VWC calculated from Topp model and ground truth measurements with Di-Sense VWC. Similarly, Fig. 9.6(c) compares Di-Sense permittivity with Peplinski model, and Fig. 9.6(d) compares the

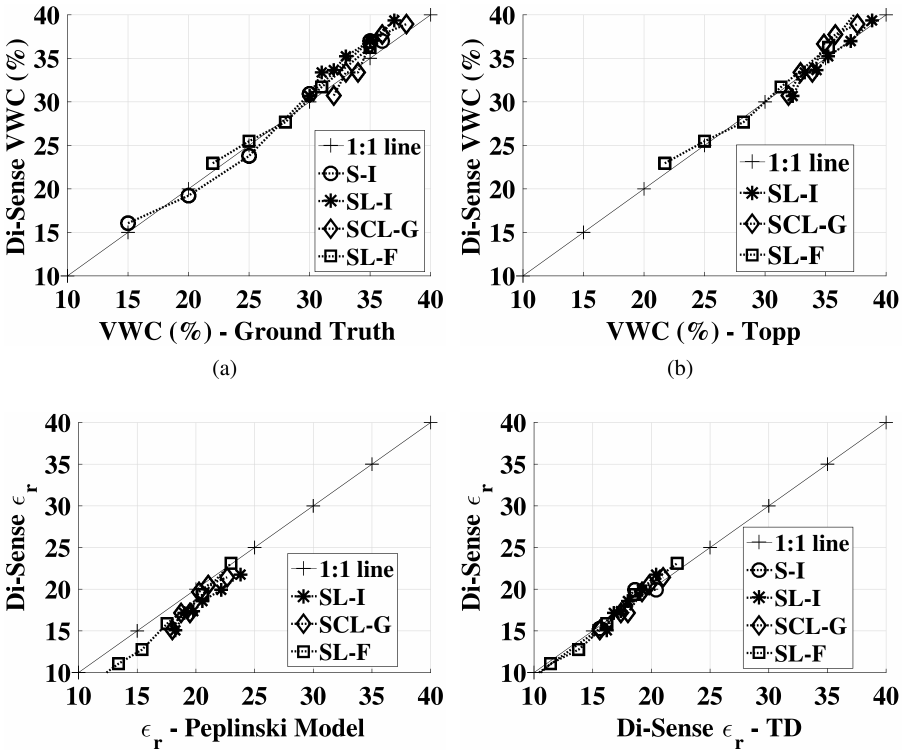

(a) (b) (c) (d)

Fig. 9.6: Comparison of VWC of Di-Sense Model with [55]: (a) VWC measure from experiments, (b) VWC from Topp model; (c) Comparison of permittivity of Di-Sense Model with permittivity from Peplinski model [55], (d) Comparison of permittivity from Di-Sense Model from time-domain velocity of propagation method with Di-Sense permittivity from path loss propagation method [55]

the Di-Sense permittivity estimated by time-domain velocity of propagation method with Di-Sense path loss propagation permittivity method. The graphs confirms the result from Di-Sense model with ground truth measurements. There are some interesting point to consider from Fig. 9.6, e.g., decrease in lowest path loss frequency causes increase in soil permittivity leading to increase in soil moisture.

9.5.3 Model Error Analysis

Figs. 9.7 shows the result from the model error analysis. Di-Sense VWC estimation error is compared with ground truth soil moisture sensing in Fig. 9.7(a). It can be observed that the error varies more in silt loam soil (1% - 8%) as compared to the

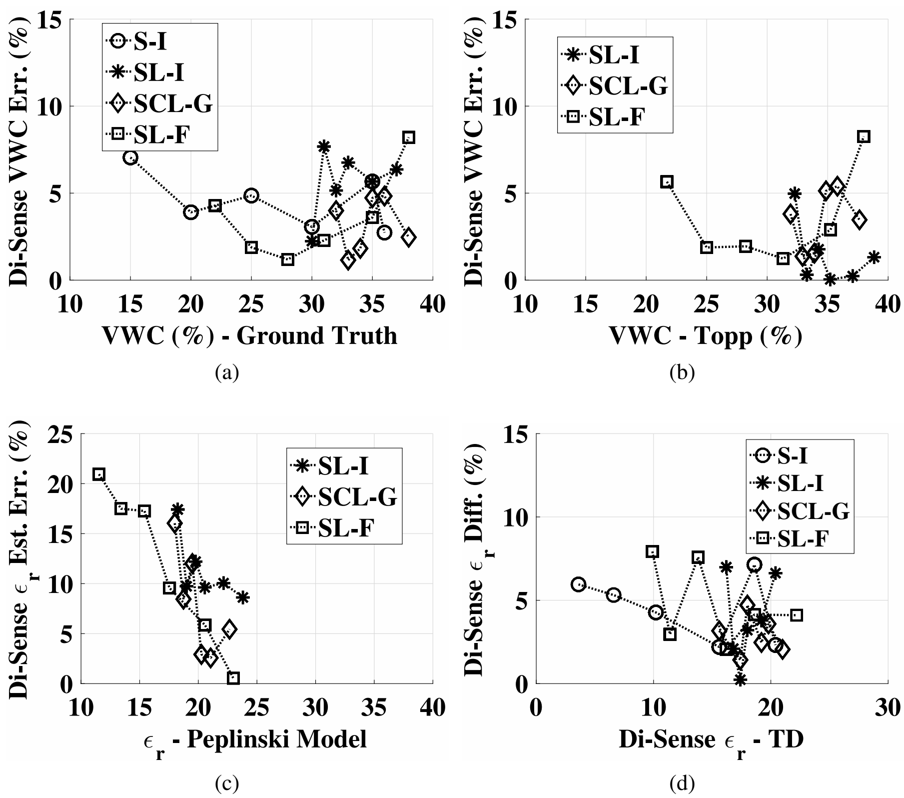

Fig. 9.7: Error Analysis of Di-Sense Model [55]: (a) comparison of VWC from Di-Sense Model with VWC measured from experiments, (b) comparison of VWC from Di-Sense Model with VWC from Topp model, (c) Comparison of permittivity of Di-Sense Model with permittivity from Peplinski model, and (d) Comparison of permittivity from Di-Sense Model from time-domain velocity of propagation method with Di-Sense permittivity from path loss propagation method

sandy soil underscoring the importance of clay contents in soil. Overall estimation error remains less than 8%.

Fig. 9.7(b) compares the Di-Sense soil moisture estimation error with that of from Topp model. As in the case of Di-Sense VWC estimation error, Di-Sense soil moisture estimation error also varies more in silt loam soil. Moreover, Di-Sense soil moisture estimation error is 7% less than the one measured from Topp model.

Fig. 9.7(c) shows the permittivity estimation error from Di-Sense and Peplinski model. It can be seen that, in comparison with Peplinski model, Di-Sense estimation error is high (21%) for silt loam (field) than silt loam (error < 15%) and silty clay loam. It can be observed that error is inversely proportional to the soil moisture levels, i.e., low error is observed for the high soil moisture. Water permittivity depends upon numerous factors, therefore, soil dielectric constant becomes complicated under high

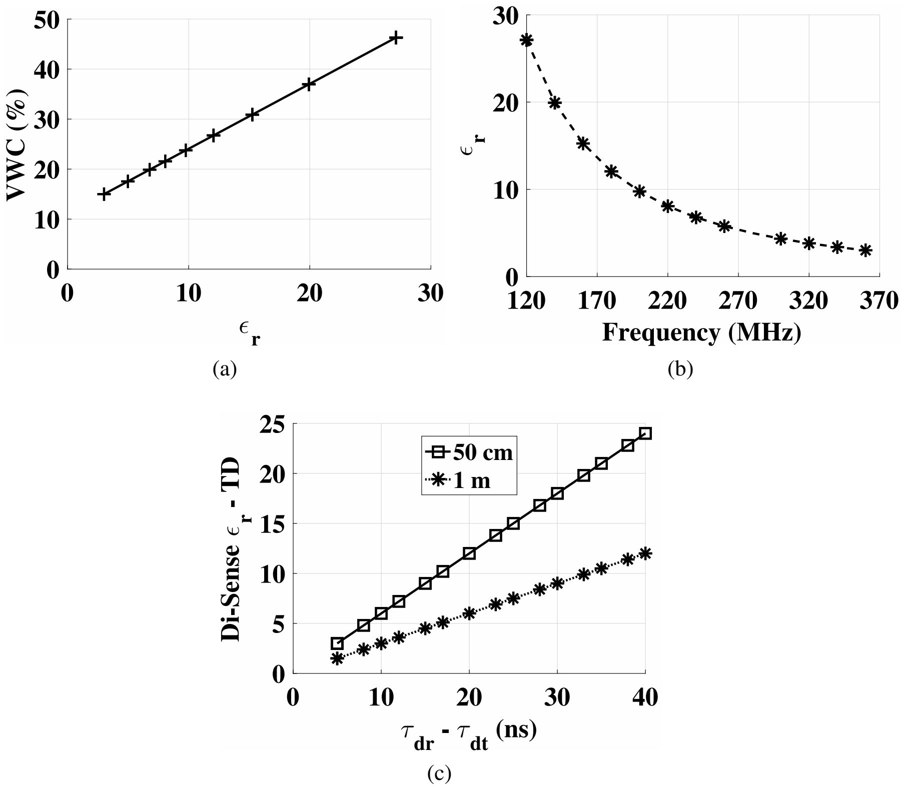

Fig. 9.8: Transfer function of Di-Sense model for [55]: (a) soil moisture, (b) soil permittivity (time-domain) (c) soil permittivity

soil moisture level. Moreover, soil permittivity also rely on many other factors such as soil temperature, soil type/texture, percentage of clay particles, bulk density, soil bulk density, porosity, and salinity. For Di-Sense soil moisture estimation model, the e ect of these factor is very low. To summarize, modeled and measured values are confirmation with each other and Di-Sense method can be considered as a feasible method for measuring soil permittivity and soil water content [26, 35].

An important thing to note is that Fig. 9.6(c) does not compare permittivity for sandy soil using Peplinski model. The reason is that Peplinski model does not work well with the sandy soil having sand content of 86% [26]. Fig. 9.7(d) shows the di erence between Di-Sense path loss propagation permittivity method and Di-Sense permittivity by time-domain velocity of propagation method and both methods are in confirmation with testbed soil with estimation di erence of less than 8%. Hence, Di-Sense model for estimating soil permittivity and soil moisture are suitable for the soils having same particle size classification and distribution as of used in these experiments [48, 55].

9.5.4 Transfer Functions of Di-Sense

Although result are most relevant for determining soil permittivity and soil moisture, however, it is also suitable for designing IOUT communication system. Moreover, soil permittivity is less e ected at higher depths because the intensity of reflected wave from soil-air interface is reduced at higher depths. Following procedure is used for estimation:

- First, lowest path loss frequency is measured.
- Soil permittivity is determined by using equations (9.5) and (9.6).
- Soil moisture is estimated by using equation (9.7).

Fig. 9.8 shows the Di-Sense transfer functions for soil moisture and soil permittivity. These graphs can be used for measuring the permittivity and soil moisture for a given IOUT propagation path loss. Di-Sense measurement method is very simple which requires no knowledge of IOUT deployment parameters, i.e., type of radios, antenna knowledge, and communication parameters. Only requirement is to accurately measure the propagation path loss. It can be used with di erent operation frequencies f_0 as equations (9.3) and (9.4)scales with the f_0. Di-Sense have some limitations as well: it requires accurate measurement of propagation path loss of soil under observation. For applications requiring higher accuracy, soil-water retention capability and specific soil properties can be represented by an empirical factor [51].

9.6 Di-Sense Applications

Di-Sense can be used for irrigation scheduling in IOUT-based agricultural systems [9]. In construction-based IOUT systems (building and bridges), Di-Sense can be used to examine the health of the building structure. In geophysical applications, Di-Sense can be used for estimating permittivity of ice and rocks. It can also be used in detection soil contamination, and in the domains of meteorology, geophysics and civil engineering.

References

[1] Abrudan TE, Kypris O, Trigoni N, Markham A (2016) Impact of rocks and minerals on underground magneto-inductive communication and localization. IEEE Access 4:3999–4010, DOI 10.1109/ACCESS.2016.2597641
[52] Akyildiz IF, Stuntebeck EP (2006) Wireless underground sensor networks: Research challenges. Ad Hoc Networks Journal
[3] Bobrov P, Repin A, Rodionova O (2015) Wideband frequency domain method of soil dielectric property measurements. Geoscience and Remote Sensing, IEEE Transactions on 53(5):2366–2372, DOI 10.1109/TGRS.2014.2359092

[58] Bogena HR, Herbst M, Huisman JA, Rosenbaum U, Weuthen A, Vereecken H (2010) Potential of wireless sensor networks for measuring soil water content variability. Vadose Zone Journal

[5] Comite D, Galli A, Lauro SE, Mattei E, Pettinelli E (2016) Analysis of gpr early-time signal features for the evaluation of soil permittivity through numerical and experimental surveys. IEEE Journal of Selected Topics in Applied Earth Observations and Remote Sensing 9(1):178–187, DOI 10.1109/JSTARS.2015.2466174

[6] Curtis JO (2001) A durable laboratory apparatus for the measurement of soil dielectric properties. IEEE Transactions on Instrumentation and Measurement 50(5):1364–1369, DOI 10.1109/19.963211

[7] Dobson M, etal (1985) Microwave dielectric behavior of wet soil—Part II: Dielectric mixing models. IEEE Trans Geoscience and Remote Sensing GE-23(1):35 –46, DOI 10.1109/TGRS.1985.289498

[9] Dong X, Vuran MC, Irmak S (2012) Autonomous precision agricultrue through integration of wireless underground sensor networks with center pivot irrigation systems. Ad Hoc Networks (Elsevier)

[9] Ettus Research Website (2016) URL `http://www.ettus.com`

[10] GNU Radio Website (2020) URL `http://www.gnuradio.org`

[75] Guo H, Sun Z (2014) Channel and energy modeling for self-contained wireless sensor networks in oil reservoirs. IEEE Trans Wireless Communications 13(4):2258–2269, DOI 10.1109/TWC.2013.031314.130835

[12] Hipp JE (1974) Soil electromagnetic parameters as functions of frequency, soil density, and soil moisture. Proceedings of the IEEE 62(1):98–103, DOI 10.1109/PROC.1974.9389

[13] Hislop G (2015) Permittivity estimation using coupling of commercial ground penetrating radars. IEEE Transactions on Geoscience and Remote Sensing 53(8):4157–4164, DOI 10.1109/TGRS.2015.2392110

[14] Irmak S, etal (2012) Large scale on-farm implementation of soil moisture-based irrigation management strategies for increasing maize water productivity. Transactions of the ASABE 55(3):881–894

[15] Irmak S, Haman D (2001) Performance of the watermark. granular matrix sensor in sandy soils. Applied Engineering in Agriculture 17(6):787

[16] Irmak S, Irmak A (2005) Performance of frequency-domain reflectometer, capacitance, and psuedo-transit time-based soil water content probes in four coarse-textured soils. Applied engineering in agriculture 21(6):999–1008

[17] Irmak S, Payero JO, Eisenhauer DE, Kranz WL, Martin D, Zoubek GL, Rees JM, VanDeWalle B, Christiansen AP, Leininger D (2006) Ec06-783 watermark granular matrix sensor to measure soil matric potential for irrigation management

[18] Jonard F, Weihermüller L, Schwank M, Jadoon KZ, Vereecken H, Lambot S (2015) Estimation of hydraulic properties of a sandy soil using ground-based active and passive microwave remote sensing. IEEE Transactions on Geoscience and Remote Sensing 53(6):3095–3109, DOI 10.1109/TGRS.2014.2368831

[19] Josephson B, Blomquist A (1958) The influence of moisture in the ground, temperature and terrain on ground wave propagation in the vhf-band. IRE

Transactions on Antennas and Propagation 6(2):169–172, DOI 10.1109/TAP.1958.1144574

[20] b Kim S, Ouellette JD, van Zyl JJ, Johnson JT (2016) Detection of inland open water surfaces using dual polarization l-band radar for the soil moisture active passive mission. IEEE Transactions on Geoscience and Remote Sensing 54(6):3388–3399, DOI 10.1109/TGRS.2016.2517010

[21] Ledieu J, Ridder PD, Clerck PD, Dautrebande S (1986) A method of measuring soil moisture by time-domain reflectometry. Journal of Hydrology 88(3):319 – 328, DOI http://dx.doi.org/10.1016/0022-1694(86)90097-1

[100] Markham A, Trigoni N (2012) Magneto-inductive networked rescue system (miners): Taking sensor networks underground. In: Proceedings of the 11th ICPS, ACM, IPSN '12, pp 317–328, DOI 10.1145/2185677.2185746

[23] MATLAB (2020) URL `http://wwwmatlab.com`

[24] Nassar EM, Lee R, Young JD (1999) A probe antenna for in situ measurement of the complex dielectric constant of materials. IEEE Transactions on Antennas and Propagation 47(6):1085–1093, DOI 10.1109/8.777136

[25] Nicolson AM, Ross GF (1970) Measurement of the intrinsic properties of materials by time-domain techniques. IEEE Transactions on Instrumentation and Measurement 19(4):377–382, DOI 10.1109/TIM.1970.4313932

[26] Peplinski N, Ulaby F, Dobson M (1995) Dielectric properties of soil in the 0.3–1.3 ghz range. IEEE Transactions on Geoscience and Remote Sensing 33(3):803–807

[27] Peplinski NR, Ulaby FT, Dobson MC (1995) Dielectric properties of soils in the 0.3-1.3-ghz range. IEEE transactions on Geoscience and Remote sensing 33(3):803–807

[28] Pettinelli E, Matteo AD, Mattei E, Crocco L, Soldovieri F, Redman JD, Annan AP (2009) Gpr response from buried pipes: Measurement on field site and tomographic reconstructions. IEEE Transactions on Geoscience and Remote Sensing 47(8):2639–2645, DOI 10.1109/TGRS.2009.2018301

[24] Salam A (2018) Pulses in the sand: Long range and high data rate communication techniques for next generation wireless underground networks. ETD collection for University of Nebraska - Lincoln (AAI10826112), URL `http://digitalcommons.unl.edu/dissertations/AAI10826112`

[26] Salam A (2019) Design of subsurface phased array antennas for digital agriculture applications. In: Proc. 2019 IEEE International Symposium on Phased Array Systems and Technology (IEEE Array 2019), Waltham, MA, USA

[27] Salam A (2019) A path loss model for through the soil wireless communications in digital agriculture. In: 2019 IEEE International Symposium on Antennas and Propagation, IEEE, pp 1–2

[28] Salam A (2019) Sensor-free underground soil sensing. In: ASA, CSSA and SSSA International Annual Meetings (2019), ASA-CSSA-SSSA

[29] Salam A (2019) Subsurface mimo: A beamforming design in internet of underground things for digital agriculture applications. Journal of Sensor and Actuator Networks 8(3), DOI 10.3390/jsan8030041, URL `https://www.mdpi.com/2224-2708/8/3/41`

[30] Salam A (2019) Underground Environment Aware MIMO Design Using Transmit and Receive Beamforming in Internet of Underground Things, Springer International Publishing, Cham, pp 1–15
[31] Salam A (2019) An underground radio wave propagation prediction model for digital agriculture. Information 10(4):147
[34] Salam A (2020) Internet of Things for Sustainability: Perspectives in Privacy, Cybersecurity, and Future Trends, Springer International Publishing, Cham, pp 299–327. DOI 10.1007/978-3-030-35291-2_10, URL https://doi.org/10.1007/978-3-030-35291-2_10
[35] Salam A (2020) Internet of Things for Sustainable Community Development, 1st edn. Springer Nature, DOI 10.1007/978-3-030-35291-2
[36] Salam A (2020) Internet of Things for Sustainable Community Development: Introduction and Overview, Springer International Publishing, Cham, pp 1–31. DOI 10.1007/978-3-030-35291-2_1, URL https://doi.org/10.1007/978-3-030-35291-2_1
[37] Salam A (2020) Internet of Things for Sustainable Forestry, Springer International Publishing, Cham, pp 147–181. DOI 10.1007/978-3-030-35291-2_5, URL https://doi.org/10.1007/978-3-030-35291-2_5
[38] Salam A (2020) Internet of Things for Sustainable Human Health, Springer International Publishing, Cham, pp 217–242. DOI 10.1007/978-3-030-35291-2_7, URL https://doi.org/10.1007/978-3-030-35291-2_7
[39] Salam A (2020) Internet of Things for Sustainable Mining, Springer International Publishing, Cham, pp 243–271. DOI 10.1007/978-3-030-35291-2_8, URL https://doi.org/10.1007/978-3-030-35291-2_8
[42] Salam A (2020) Internet of Things in Sustainable Energy Systems, Springer International Publishing, Cham, pp 183–216. DOI 10.1007/978-3-030-35291-2_6, URL https://doi.org/10.1007/978-3-030-35291-2_6
[43] Salam A (2020) Internet of Things in Water Management and Treatment, Springer International Publishing, Cham, pp 273–298. DOI 10.1007/978-3-030-35291-2_9, URL https://doi.org/10.1007/978-3-030-35291-2_9
[44] Salam A (2020) Wireless underground communications in sewer and stormwater overflow monitoring: Radio waves through soil and asphalt medium. Information 11(2)
[45] Salam A, Karabiyik U (2019) A cooperative overlay approach at the physical layer of cognitive radio for digital agriculture
[46] Salam A, Shah S (2019) Internet of things in smart agriculture: Enabling technologies. In: 2019 IEEE 5th World Forum on Internet of Things (WF-IoT), IEEE, pp 692–695
[139] Salam A, Vuran MC (2016) Impacts of soil type and moisture on the capacity of multi-carrier modulation in internet of underground things. In: Proc. ICCCN 2016, Waikoloa, Hawaii, USA

[47] Salam A, Vuran MC (2016) Impacts of soil type and moisture on the capacity of multi-carrier modulation in internet of underground things. In: Proc. of the 25th ICCCN 2016, Waikoloa, Hawaii, USA

[48] Salam A, Vuran MC (2017) Em-based wireless underground sensor networks pp 247–285, DOI 10.1016/B978-0-12-803139-1.00005-9

[50] Salam A, Vuran MC (2017) Smart underground antenna arrays: A soil moisture adaptive beamforming approach. In: Proc. 36th IEEE INFOCOM 2017, Atlanta, USA

[49] Salam A, Vuran MC (2017) Smart underground antenna arrays: A soil moisture adaptive beamforming approach. In: Proc. IEEE INFOCOM 2017, Atlanta, USA

[50] Salam A, Vuran MC (2017) Wireless underground channel diversity reception with multiple antennas for internet of underground things. In: Proc. IEEE ICC 2017, Paris, France

[145] Salam A, Vuran MC, Irmak S (2016) Pulses in the sand: Impulse response analysis of wireless underground channel. In: Proc. IEEE INFOCOM 2016, San Francisco, USA

[51] Salam A, Vuran MC, Irmak S (2016) Pulses in the sand: Impulse response analysis of wireless underground channel. In: The 35th Annual IEEE International Conference on Computer Communications (INFOCOM 2016), San Francisco, USA

[52] Salam A, Vuran MC, Irmak S (2017) Towards internet of underground things in smart lighting: A statistical model of wireless underground channel. In: Proc. 14th IEEE International Conference on Networking, Sensing and Control (IEEE ICNSC), Calabria, Italy

[53] Salam A, Hoang AD, Meghna A, Martin DR, Guzman G, Yoon YH, Carlson J, Kramer J, Yansi K, Kelly M, et al. (2019) The future of emerging iot paradigms: Architectures and technologies

[55] Salam A, Vuran MC, Irmak S (2019) Di-sense: In situ real-time permittivity estimation and soil moisture sensing using wireless underground communications. Computer Networks 151:31 – 41, DOI https://doi.org/10.1016/j.comnet.2019.01.001, URL `http://www.sciencedirect.com/science/article/pii/S1389128618303141`

[58] Scott WR, Smith GS (1992) Measured electrical constitutive parameters of soil as functions of frequency and moisture content. IEEE Transactions on Geoscience and Remote Sensing 30(3):621–623, DOI 10.1109/36.142943

[59] Small EE, Larson KM, Chew CC, Dong J, Ochsner TE (2016) Validation of gps-ir soil moisture retrievals: Comparison of di erent algorithms to remove vegetation e ects. IEEE Journal of Selected Topics in Applied Earth Observations and Remote Sensing 9(10):4759–4770, DOI 10.1109/JSTARS.2015.2504527

[60] Smith G, Nordgard J (1985) Measurement of the electrical constitutive parameters of materials using antennas. IEEE Transactions on Antennas and Propagation 33(7):783–792, DOI 10.1109/TAP.1985.1143657

[61] Smith GS, King RWP (1974) The resonant linear antenna as a probe for measuring the in situ electrical properties of geological media. Journal of

Geophysical Research 79(17):2623–2628, DOI 10.1029/JB079i017p02623, URL http://dx.doi.org/10.1029/JB079i017p02623

[62] Solimene R, D'Alterio A, Gennarelli G, Soldovieri F (2014) Estimation of soil permittivity in presence of antenna-soil interactions. IEEE Journal of Selected Topics in Applied Earth Observations and Remote Sensing 7(3):805–812, DOI 10.1109/JSTARS.2013.2268576

[170] Tan X, Sun Z, Akyildiz IF (2015) Wireless underground sensor networks: MI-based communication systems for underground applications. IEEE Antennas and Propagation Magazine 57(4), DOI 10.1109/MAP.2015.2453917

[65] Temel S, Vuran MC, Lunar MM, Zhao Z, Salam A, Faller RK, Stolle C (2018) Vehicle-to-barrier communication during real-world vehicle crash tests. Computer Communications 127:172–186

[104] Tiusanen MJ (2013) Soil scouts: Description and performance of single hop wireless underground sensor nodes. Ad Hoc Networks 11(5):1610 – 1618, DOI http://dx.doi.org/10.1016/j.adhoc.2013.02.002

[66] Topp GC, Davis JL, Annan AP (1980) Electromagnetic determination of soil water content: Measurements in coaxial transmission lines. Water Resources Research 16(3):574–582, DOI 10.1029/WR016i003p00574

[67] Toro-Vazquez J, Rodriguez-Solis RA, Padilla I (2012) Estimation of electromagnetic properties in soil testbeds using frequency and time domain modeling. IEEE Journal of Selected Topics in Applied Earth Observations and Remote Sensing 5(3):984–989, DOI 10.1109/JSTARS.2012.2193610

[68] Ulaby FT, Long DG (2014) Microwave Radar and Radiometric Remote Sensing. University of Michigan Press

[69] van der Velde R, Salama MS, Eweys OA, Wen J, Wang Q (2015) Soil moisture mapping using combined active/passive microwave observations over the east of the netherlands. IEEE Journal of Selected Topics in Applied Earth Observations and Remote Sensing 8(9):4355–4372, DOI 10.1109/JSTARS.2014.2353692

[70] Vereecken H, Schnepf A, Hopmans JW, Javaux M, Or D, Roose T, Vanderborght J, Young M, Amelung W, Aitkenhead M, et al. (2016) Modeling soil processes: Review, key challenges, and new perspectives. Vadose Zone Journal 15(5)

[71] Vuran MC, Dong X, Anthony D (2015) Antenna for wireless underground communication. URL http://www.google.com/patents/US20150181315, uS Patent App. 14/415,455

[71] Vuran MC, Salam A, Wong R, Irmak S (2018) Internet of underground things in precision agriculture: Architecture and technology aspects. Ad Hoc Networks DOI https://doi.org/10.1016/j.adhoc.2018.07.017, URL http://www.sciencedirect.com/science/article/pii/S1570870518305067

[72] Vuran MC, Salam A, Wong R, Irmak S (2018) Internet of underground things: Sensing and communications on the field for precision agriculture. In: 2018 IEEE 4th World Forum on Internet of Things (WF-IoT) (WF-IoT 2018), , Singapore

[74] Wang JR, Schmugge TJ (1980) An empirical model for the complex dielectric permittivity of soils as a function of water content. IEEE Transactions on

Geoscience and Remote Sensing GE-18(4):288–295, DOI 10.1109/TGRS.1980.350304

[75] Weir WB (1974) Automatic measurement of complex dielectric constant and permeability at microwave frequencies. Proceedings of the IEEE 62(1):33–36, DOI 10.1109/PROC.1974.9382

[76] Welch PD (1967) The use of fast fourier transform for the estimation of power spectra: A method based on time averaging over short, modified periodograms. Audio and Electroacoustics, IEEE Transactions on 15(2):70–73, DOI 10.1109/TAU.1967.1161901